



Olefin Upgrading over Ir/ZSM-5 catalysts under methane environment

Yang Lou, Peng He, Lulu Zhao, Wei Cheng, Hua Song*

Department of Chemical and Petroleum Engineering, University of Calgary, 2500 University Dr NW, Calgary, Alberta T2N 1N4, Canada

ARTICLE INFO

Article history:

Received 12 March 2016

Received in revised form 17 August 2016

Accepted 19 August 2016

Available online 21 August 2016

Keywords:

Methane activation

Bifunctional catalysts

Ir/ZSM-5

Olefin upgrading

Hydrogen donor

ABSTRACT

Upgrading olefin in the synthetic oil to alkane is highly desired due to its high volatility and thermal instability as well as low energy density. Unlike conventional hydrotreating, methane (CH_4) was used in this study as the novel hydrogen donor for olefin saturation. The significant increase of H/C atomic ratio of product oil from 1.69 ± 0.02 (over pure ZSM-5) to 2.04 ± 0.02 (over Ir/ZSM-5 (10.0)) and the alkane content up to $83.8 \pm 2.1\%$ in the upgraded oil indicated that methane could exhibit comparable catalytic performance to what hydrogen (H_2) did for olefin (1-Decene) upgrading over the developed bifunctional catalysts with low Ir loadings. The HRTEM and XPS data revealed that the highly dispersed metallic Ir particles with average size of 1.32 nm was coexisting with IrO_2 species. The synergic effects of Ir/ IrO_2 obviously promoted the activation of methane, which supplied sufficient hydrogen for the saturation and stabilization of olefin. The results from BET indicated that the pore size and volume of the ZSM-5 support were increased upon Ir introduction, which provided more active sites for cracking olefin (1-decene). NH₃-TPD results suggested that the presence of highly dispersed Ir increased the amount of surface acidity, which enhanced the formation and stabilization of carbenium ion intermediates. As a result, the produced alkanes were mainly composed of cyclopentane-derived compounds, like propylcyclopentane, 3-methylbutyl-cyclopentane and 1,2,4-trimethyl-cyclopentane, which has great application potential as immersion fluid and additive in the field of optics and petroleum.

© 2016 Elsevier B.V. All rights reserved.

1. Introduction

Olefins including light and long-chain unsaturated compounds are abundant byproducts of catalytic cracking [1] and Fisher-Tropsch synthesis [2] but are underutilized as energy carriers because of their high volatility and low energy density [3]. In addition, the presence of olefin could not only cause the formation of polymeric deposit due to its thermal instability during long-term storage and long distance transportation but also lead to gasoline insufficient combustion, generating negative environmental impact. Therefore, upgrading olefin to alkane is critical not only for the enhancement of product stability but also for the protection of our environment. Generally, hydrotreating is widely employed to saturate olefins for the improvement of gasoline quality [4,5]. However, the involvement of hydrogen (H_2) obviously increases the cost of this upgrading step since H_2 is not naturally available. Current steam reforming of natural gas (mainly composed of CH_4) accounts for almost 50% of the world feedstock for hydrogen (H_2) production but is operated in a high temperature range of 973–1173 K

[6,7], which not only increases the operation cost but also leads to huge emission of CO_2 . Hence, if methane could be directly used as the novel hydrogen donor and act as an alternative to expensive hydrogen gas for olefin upgrading, not only the operation costs but also greenhouse gas emission could be significantly reduced.

Although direct activation of CH_4 is uneasy due to its symmetrically geometric and stable electronic structure [8,9], the previous research reveals that the methane could be efficiently activated over bifunctional catalysts [10–14] (M/zeolites, M: metal species) in the presence of alkene and higher alkane at near atmospheric pressure and mild temperature (400–600 °C). For instance, the presence of n-butene could efficiently facilitate CH_4 conversion up to 45.0% at 600 °C and 1 atm, which produces not only high value products of aromatics and H_2 but also exhibits high selectivity toward aromatics (up to 92.0%) formation [10]. From the aspect of thermodynamics, the reaction barrier could be significantly reduced to zero or even negative when methane reacts with alkenes or higher alkanes under appropriate conditions; for example, the positive Gibbs free energy change (ΔG_f) value of direct formation of benzene from methane could become -4.1 kcal/mol at 500 °C and -10.6 kcal/mol at 600 °C when the ratio of n-butene/methane was 1.0 [10]. Moreover, Har [4] and Song et al. [15–18] reported that methane could act as comparable or even better hydrogen donors

* Corresponding author.

E-mail address: sonh@ucalgary.ca (H. Song).

than H₂ for upgrading heavy oil and crude bio-oil during biomass pyrolysis. Hence, CH₄ could be employed as a novel hydrogen donor for olefin upgrading from both theoretical and practical viewpoints.

On the surface acidic centers of bifunctional catalysts, olefin could be cracked down through α -C-C scission and β -C-C scission to smaller molecules [19–22], which contain unsaturated hydrocarbons featured by the presence of C=C and C≡C bonds in their molecular structures. Surface acidic centers could easily catalyze the unsaturated bonds to form the carbenium ions [20,23], which are highly reactive fragments for further agglomeration, isomerization, cyclization, hydrogen redistribution and so on [24–26].

Therefore, it would be a feasible and efficient method to saturate olefin by CH₄ over well-developed bi-functional catalysts based on the aforementioned reaction between methane and co-existing unsaturated hydrocarbons. In the meantime, the reaction between activated CH₄ and highly reactive fragments formed after olefin cracking would efficiently increase the H/C atomic ratio and alkane contents of product oil, which could not only make the product oil more stable but also efficiently inhibit the formation of coke during its further processing and application. In addition, the formed CH_x moiety from methane activation might be incorporated into the upgraded oil product, leading to the enhancement of oil yield. Shortly, taking methane as a novel hydrogen donor would not only effectively reduce the greenhouse emission and operation costs for olefin upgrading but also supply a novel way for CH₄ utilization, which could make olefin upgrading more economically attractive and environmentally friendly.

Ir-based catalysts are widely used and studied in the fields of environment and fundamental researches [27–30]. Both of Ir and IrO₂ species exhibit excellent capability of C–H bonds activation of CH₄ [3,31–35]. IrO₂ could exhibit very high reactivity for methane activation because the electron density transfer from the d_{z²} orbital of coordinatedly unsaturated Ir (Ir_{cu}) atom to C–H bond could weaken the C–H bond of CH₄ through the interaction between the σ bond of C–H of CH₄ and the Ir_{cu} atoms [33]. The activation energy for methane dissociative chemisorption on Ir (111) could be as low as 15 kJ/mol [35]. Furthermore, C–H bond activation is the only kinetically limiting step in CH₄ activation on supported Ir species, the reactivity of which increases with increasing dispersion of Ir species [32]. Therefore, the supply of hydrogen donors could be promoted with the increase of Ir dispersion, which would enhance the saturation of carbenium ions [20].

Hence, in this paper, highly dispersed Ir/ZSM-5 bifunctional catalysts are synthesized by the deposition precipitation method (DP). The prepared highly-dispersed Ir catalysts not only significantly lower the loadings of noble metal and promote methane activation but also appropriately tune the surface acidity of ZSM-5, which could supply sufficient hydrogen donors and efficiently modulate the catalytic cracking for olefin upgrading.

2. Experimental

2.1. Synthesis of the catalysts

Unlike the conventional Ir catalysts mainly prepared by impregnation methods, which have Ir particles poorly dispersed on and weakly interacted with support, the Iridium catalysts developed in this research were prepared using the following procedures [18,36–39], which could strengthen the interactions between Ir metal particles and the zeolite supports. An IrCl₃ (Sigma, 99.8%) aqueous solution with concentration of 1.0 mmol/L was dropwisely introduced into a 200 mL aqueous solution suspended with HZSM-5 powder manufactured by Zeolyst® (2.0 g, activated at 600 °C in air for 5 h) under stirring. The pH of the resulting solution was adjusted to set values using aqueous solutions of HCl and NaOH.

The SiO₂/Al₂O₃ (Si/Al) ratio of ZSM-5 used in our experiment was 80:1 unless otherwise stated. The resultant slurry was further aged at room temperature for 2 h and was then washed with distilled water for several times. The achieved solid material was dried at 80 °C for 12 h and calcined in air at 400 °C for 2 h.

It is widely recognized that the dispersion of a noble metal on a support is prominently influenced by the affinity of its precursor to the support and strong affinity could facilitate its good dispersion [40]. Therefore, different pH values (pH = 7.0, 8.0, 9.0 and 10.0) were chosen to prepare the well-dispersed Ir mounted onto ZSM-5 support according to the aforementioned synthesis recipe. And the corresponding catalysts were named as Ir/ZSM-5 (x), where x was pH value. The Ir actual loadings of these samples were 0.11 wt.%, 0.19 wt.%, 0.18 wt.% and 0.26 wt.%, respectively, when the preparation pH values were chosen at 7.0, 8.0, 9.0 and 10.0. The reported loading of Ir here was measured by ICP-AES (Varian 710). In order to investigate the effects of surface acidity on the catalytic performance, Ir/ZSM-5 catalysts with Si/Al ratio of 50:1 and 280:1 were also prepared following the same procedure as that of Ir/ZSM-5 (80:1, 10.0) and the corresponding loadings of Ir were 0.30 wt.% and 0.21 wt.% for Ir/ZSM-5 (50:1) and Ir/ZSM-5 (280:1), respectively.

2.2. Catalytic performance evaluation

1-Decene (C₁₀H₂₀, Alfa, 96%) was used as the model compound of olefin to evaluate the catalytic performance of catalysts prepared for olefin upgrading. The activity of catalysts was evaluated in a batch reactor (300 mL, Parr Instrument Co.). 8.5 g 1-decene was mixed with 0.085 g Ir/ZSM-5 catalyst and charged into the batch reactor. 30 bar CH₄ was introduced to the reactor after purging with methane for 3 times to remove air residue. The reactants were heated to 400 °C for 40 min (different reaction time and temperature was used when otherwise mentioned). The H/C molar ratio, alkane content and heating value of the resulted product oil were measured to characterize the catalytic performance as detailed in the followings.

The CHNS elementary analysis of the liquid product was carried out using an Elemental Analyzer (Perkin Elmer 2400 Series) in order to determine the weight percentage of C and H in the liquid samples. The atomic ratio of H to C was calculated from the corresponding weight percentages with accuracy of ± 0.01 .

The heating value of the liquid product was determined by an oxygen bomb calorimeter (Parr 6100 Compensated Jacket Calorimeter). The measurement was carried out at room temperature.

The composition of the product oil was determined by the pre-calibrated Gas Chromatography-Mass Spectrometer (GC-MS: PerkinElmer GC Claus 680 and MS Clarus SQ 8T) equipped with a Paraffins-Olefins-Naphthenes-Aromatics (PONA) column (Agilent HP-PONA). The oven temperature of the GC was programmed to hold at 35 °C for 0.5 min, ramp to 200 °C at 5 °C/min, and hold for 0.5 min.

2.3. Catalyst characterization

The XRD patterns were obtained with Rigaku D/max 2550 VB/PC diffractometer using a Cu K α radiation ($\lambda = 1.54056 \text{ \AA}$). The X-ray tube was operated at 40 kV and 100 mA. The intensity data was collected at room temperature in a 2 θ range from 10° to 70° with a scan rate of 6°/min.

The N₂ adsorption–desorption isotherm analysis was measured through nitrogen adsorption at liquid nitrogen temperature by using a surface area and porosity analyzer (Quantachrome NOVA 4000e apparatus). Before measurement, the samples were degassed at 180 °C for 6 h in vacuum.

Temperature-Programmed Desorption of NH₃ (NH₃-TPD) experiments were carried out using a quartz apparatus, manufactured by our laboratory, equipped with a thermal conductivity detector (TCD) GC-15A. Prior to adsorption experiments, 100 mg of catalyst were pretreated for 1 h at 400 °C in an argon flow with a flow rate of 30 mL/min. Upon cooling to 100 °C, the samples were saturated with a pure NH₃ flow for 15 min, and then the physisorbed NH₃ were removed through purging with argon gas for 30 min. The samples were then heated to 600 °C at a heating rate of 10 °C/min in argon under a flow rate of 30 mL/min.

The X-ray photoelectron spectroscopy (XPS) was investigated in an AXIS-Ultra-DLD spectrometer (Kratos Analytical) using a monochromated Al K α X-ray source (1486.6 eV). The XPS spectra of the selected elements were measured with the constant analyzer pass energy of 80.0 eV. All binding energies (BEs) were referred to the adventitious C 1 s peak (BE = 284.6 eV). The peaks were fitted according to the Refs. [41,42].

The ²⁷Al MAS NMR spectra were acquired at room temperature on a Bruker MSL-500 spectrometer equipped with a zirconia rotor of 7 mm in diameter. The magnetic field was equal to 11.7 T and the spinning frequency was 4.0 kHz. ²⁷Al MAS NMR spectra were recorded at a resonance frequency of 130.3 MHz with a 30 μ s radiofrequency pulse, 4.6 ms excitation pulses, a recycle delay of 5.0 s and a spectral width of 29.4 kHz. The number of scan is 700 for ²⁷Al NMR spectra. The chemical shifts were referenced to AlCl₃·6H₂O for ²⁷Al. The ²⁹Si MAS NMR spectra were acquired at room temperature on an Varian Infinity Plus 400 spectrometer equipped with a Varian 7.5 mm MAS HXY probe. The samples were packed in a zirconia rotor of 7.5 mm in diameter. The magnetic field was equal to 9.4 T and the spinning frequency was 5.0 kHz. The resonance frequency of ²⁹Si was 79.4 MHz. T1 was measured by changing the tau values from 1 ms to 50 s with 20 increments. The number of scan was 40. The recycle delay was 25 s. T1 value was determined using Varian's Spinsight software by fitting the intensity of the peak to the equation $y = A \{1 - [1 + W(1 - \exp(-d_1/T_1))] \exp(-\tau/T_1)\}$, where A is the peak intensity where $\tau \gg T_1$, W is the inversion efficiency, d₁ is the recycle delay. T1 of HZSM-5 and Ir/ZSM-5 were determined to be 5.6 and 5.2 s, respectively, with an uncertainty of 0.3 s. ²⁹Si MAS NMR spectra were recorded by using one-pulse sequence with a 4.6 μ s excitation pulses ($\sim 80^\circ$ tip angle), an acquisition time of 10.24 ms, a recycle delay of 30 s, a number of scan of 400 and a spectral width of 25.0 kHz. Si-29 NMR spectra were referenced with respect to TMS by setting the high-frequency peak of tetrakis(trimethylsilyl)silane to -9.8 ppm.

High-resolution Transmission Electron Microscopy (HRTEM) images were obtained with a JOEL 2100 instrument. The specimens were prepared by ultrasonic dispersion in ethanol, evaporating a drop of the resultant suspension onto a copper support grid.

The pyridine adsorption on the catalysts was measured on a Nicolet Nexus 6700 spectrometer under a Diffuse Reflectance Infrared Fourier Transform (DRIFT) mode, which was fitted with ZnSe windows and a vacuum system. The pyridine adsorption spectra obtained were collected with a resolution of 4 cm⁻¹ and 64 scans. Prior to adsorption, the samples were pretreated in situ at 400 °C for 1 h under evacuation, then cooled to 50 °C where pyridine vapor was introduced into the cell for 0.5 h. The physically adsorbed pyridine was removed by evacuating for 1 h.

3. Results and discussions

3.1. Catalytic performance test

3.1.1. H/C ratio of product oil over different catalysts

H/C ratio is firstly used to characterize the catalytic performance of pure ZSM-5 and Ir/ZSM-5 catalysts for upgrading olefin

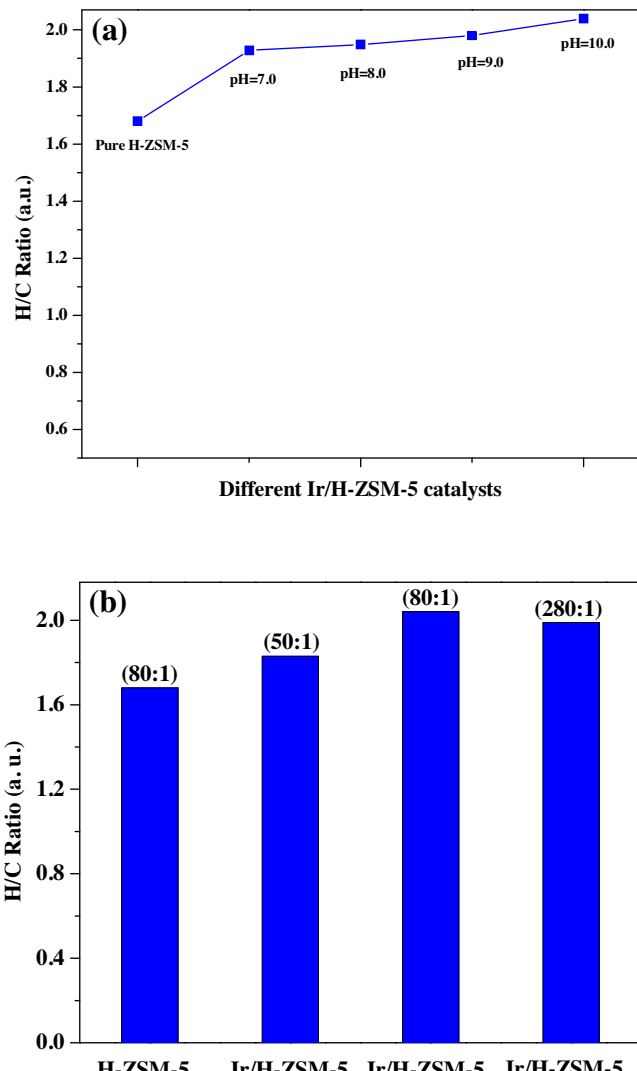


Fig. 1. H/C ratio of the oil product collected over pure ZSM-5 and Ir/ZSM-5 prepared under different pH values (a); Ir/ZSM-5 (10.0) catalysts with different Si/Al ratios (b).

to alkane under methane environment as shown in Fig. 1. It is clearly observed that the H/C ratio of product oil from pure ZSM-5 is 1.69 ± 0.02 as shown in Fig. 1(a), which is obviously lower than the ideal value of 2.2 the H/C ratio of ideal decene saturation product of decane ($C_{10}H_{22}$). The obvious decrease in the H/C ratio of the product oil might be closely related to severe cracking or formation of aromatics over pure ZSM-5, which is evidenced in the following section. However, when Ir is loaded on ZSM-5, the H/C ratio of the product oil is increased greatly. The H/C ratio of oil product is gradually increased to 2.04 ± 0.02 from 1.69 ± 0.02 (that from pure ZSM-5) when Ir/ZSM-5 (10.0) with Ir loading of 0.26 wt.% is used, which implies that the presence of low loadings of Ir on ZSM-5 could significantly promote the olefin conversion to alkane and inhibit over-cracking and aromatization of olefin. These results imply that the pH value used during Ir/ZSM-5 synthesis might affect the dispersion of Ir and the interaction between Ir and ZSM-5 support, which would significantly influence the saturation degree of olefin under methane environment.

The catalytic cracking of olefin like 1-decene is mainly influenced by the surface acidity of charged zeolite [43] that is mainly determined by its Si/Al ratio. The lower Si/Al ratio the zeolite has, the higher surface acidity it would exhibit [44]. Hence, the effect of surface acidity on the H/C ratio of product oil collected over Ir/ZSM-

5 with different Si/Al ratios prepared under pH equal to 10.0 is also investigated. As shown in Fig. 1(b), when the Si/Al ratios of the catalysts are 50 and 280, respectively, the H/C of the produced oil is higher than that from pure ZSM-5 but obviously lower than that from the catalyst with Si/Al ratio of 80. The obvious decrease in the H/C atomic ratio of the product oil might be ascribed to the formation of aromatics and/or over-cracking.

Shortly, the presence of Ir could significantly facilitate the olefin upgrading to alkane under appropriate reaction conditions, which might originate from the fact that highly dispersed Ir species could efficiently activate methane.

3.1.2. Alkane content of product oil

In order to further characterize the catalytic performance of Ir/ZSM-5 catalysts, the alkane content of product oil is quantified using the GC-MS as shown in Fig. 2. Under the same reaction conditions (400°C for 40 min), the alkane content from pure ZSM-5 (80:1) is about $2.7 \pm 0.7\%$ as shown in Fig. 2(a). The conversion of 1-decene is 100% over pure ZSM-5 but most of the oil products are in the form of benzene-based compounds and the content of aromatics is about 68.0%, which confirms the aforementioned low H/C atomic ratio of product oil from pure ZSM-5 (80:1). Meanwhile, these results not only suggest that the surface acidity of ZSM-5 is strong enough to crack the 1-decene but also indicate the weak capability for methane activation over pure ZSM-5. However, for the product oil collected from Ir/ZSM-5 catalysts, the alkane content is greatly increased with the Ir addition compared to that from ZSM-5 support. The alkane content could be up to $44.2 \pm 2.4\%$ over Ir/ZSM-5 (10.0) although the conversion of 1-decene ($96.0 \pm 0.1\%$) is lower than that from pure ZSM-5, which suggests that the presence of Ir could greatly promote the activation of methane.

In order to further illustrate the effects of surface acidity, the olefin upgrading performances of various catalysts of Ir/ZSM-5 (10.0) with different Si/Al ratios are compared and discussed in term of alkane formation. The alkane content of the product oil is about $1.4 \pm 0.2\%$ when Ir/ZSM-5 with Si/Al ratio of 280 is utilized. When the ratio of Si/Al is reduced to 50, the alkane content of the upgraded oil is increased to $10.3 \pm 2.3\%$ compared to that from Ir/ZSM-5 with Si/Al ratio of 280 but still much lower than that from Ir/ZSM-5 with optimal Si/Al ratio of 80. Moreover, for the product oil collected over Ir/ZSM-5 (50:1), the major forms of alkene are the short-chain molecules, which might be because over-strong surface acidity of Ir/ZSM-5 (50:1) makes the olefin over-cracked, generating lots of short-chain olefins.

In order to further identify the effects of reaction temperature on the alkane content of upgraded oil, the catalysts of Ir/ZSM-5 (10.0) and Ir/ZSM-5 (9.0) are investigated under different reaction temperatures. As shown in Fig. 2(c), for the Ir/ZSM-5 (10.0) catalyst, the alkane content of the product oil is increased to $83.8 \pm 2.1\%$ when the reaction temperature is decreased to 350°C , which is obviously higher than that from Ir/ZSM-5 (10.0) and pure ZSM-5 at 400°C . The produced alkanes are mainly composed of cyclopentane-derived compounds as shown in Table 1, like propylcyclopentane, 3-methylbutyl-cyclopentane and 1,2,4-trimethyl-cyclopentane, which has excellent application potential as immersion fluid and additive in the field of optics [45,46] and petroleum [47,48]. The increased alkane content of product oil from Ir/ZSM-5 (9.0) at 350°C also further evidences the effect of reaction temperature as shown in Fig. 2(c). In order to study the effect of reaction time on the alkane content of upgraded oil, the catalyst of Ir/ZSM-5 (10.0) is investigated under longer reaction time (2 h and 4 h under the same conditions used for 40 min). The testing results suggest that the over-long reaction time will slightly decrease the H/C ratio of the formed liquid products from 2.04 (40 min) to 2.02 (2 h) and 1.96 (4 h), respectively, implying that the over-long reaction time could cause the dehydrogenation of pro-

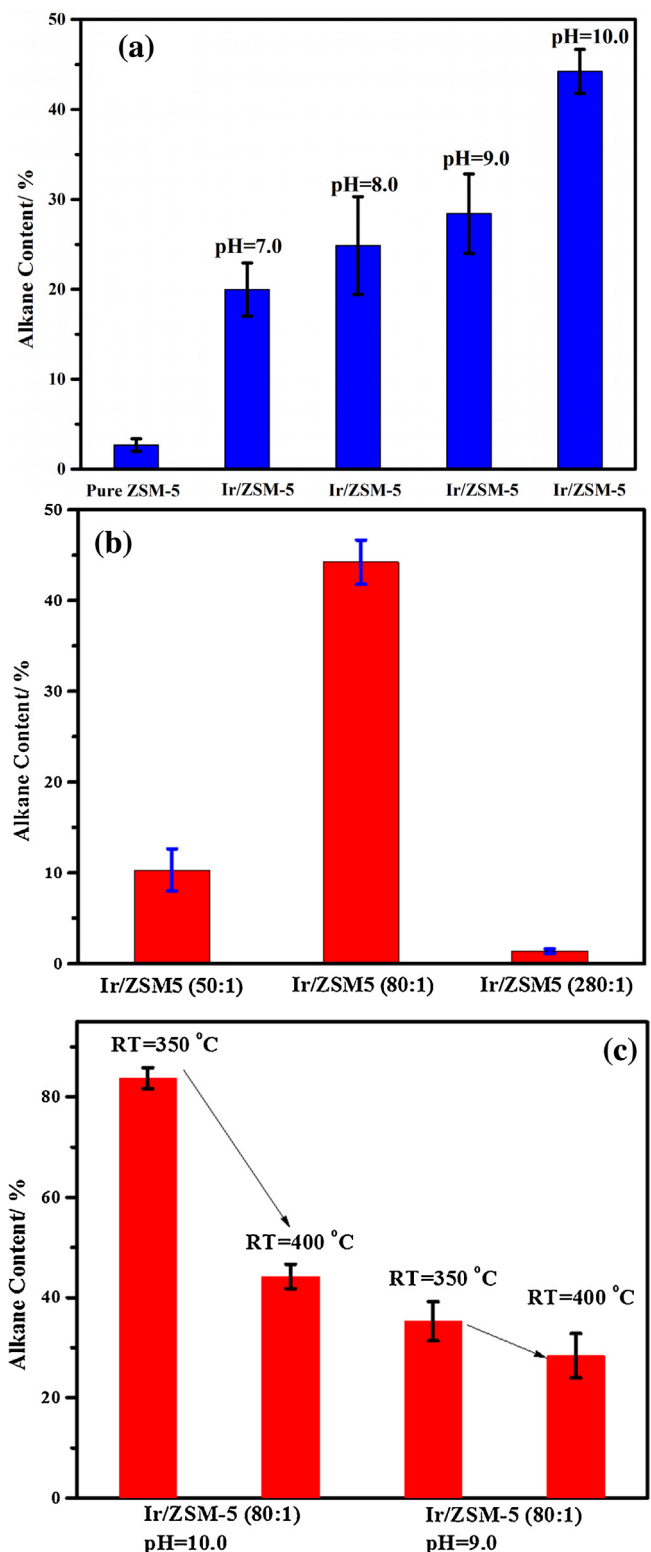


Fig. 2. Alkane content of product oil collected over pure ZSM-5 and Ir/ZSM-5 prepared under different pH values (a); Ir/ZSM-5 (10.0) catalysts with different Si/Al ratios (b); Ir/ZSM-5 (80:1, 10.0 and 9.0) under different reaction temperature (c).

duced alkane. However, the alkane content of pure ZSM-5 at 350°C is kept at about $2.8 \pm 0.6\%$, which is similar to what is observed at 400°C ($2.7 \pm 0.7\%$ as shown in Fig. 2(a)), indicating that there is no significant increase in the alkane content of product oil when the reaction temperature is decreased from 400°C to 350°C over pure

Table 1

Distribution of alkanes in the product oil from Ir/ZSM-5 (10.0) at 350 °C under methane environment.

Alkane	Formula	Content/mol.%
Cyclopentane, 1,2-dimethyl-	C ₇ H ₁₄	0.43
Cyclobutane, butyl-	C ₈ H ₁₆	0.40
Cyclopentane, 1-ethyl-3-methyl-	C ₈ H ₁₆	0.49
Cyclopentane, 1,2,3-trimethyl-	C ₈ H ₁₆	8.93
Cyclopentane, propyl-	C ₈ H ₁₆	42.33
Cyclopentane, 2-methylpropyl-	C ₉ H ₁₈	7.45
Cyclopentane, 1-methyl-2-propyl-	C ₉ H ₁₈	7.99
Cyclopentane, 3-methylbutyl-	C ₁₀ H ₂₀	10.63
Cyclopropane, 1-ethyl-2-pentyl-	C ₁₀ H ₂₀	3.91

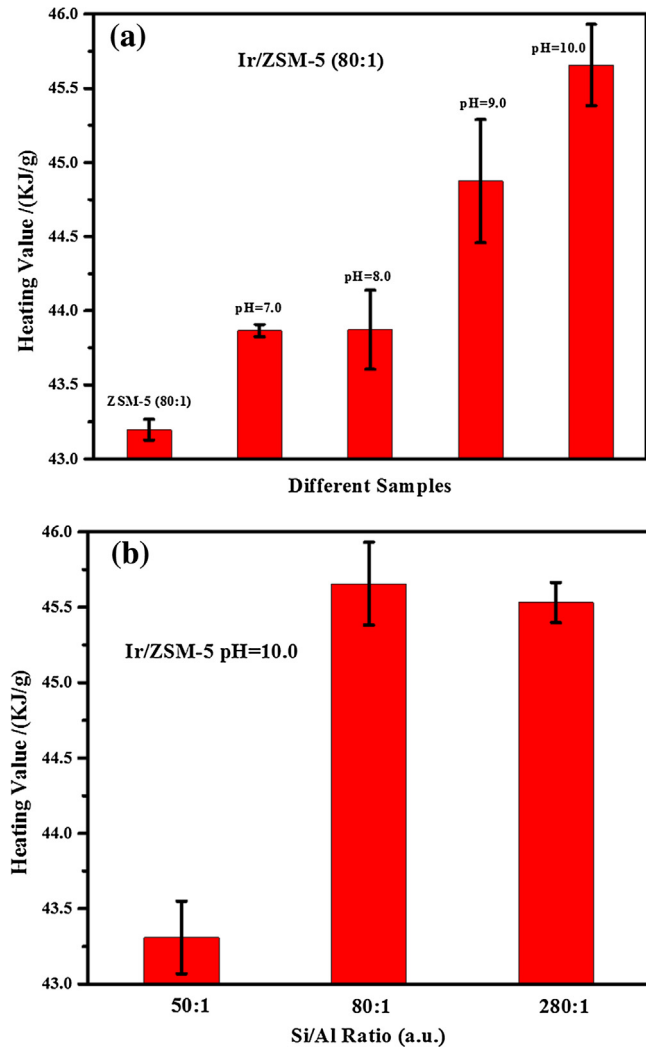


Fig. 3. Heating value of product oil collected over pure ZSM-5 and Ir/ZSM-5 prepared under different pH values (400 °C for 40 min) (a); Ir/ZSM-5 (10.0) catalysts with different Si/Al ratios (400 °C for 40 min) (b).

ZSM-5 support. This result implies the important role of Ir played on methane activation.

3.1.3. Heating value of product oil over different catalysts

As shown in Fig. 3(a), the presence of Ir could obviously promote the heating value of product oil obtained from Ir/ZSM-5 catalysts prepared under different pH values (400 °C for 40 min). The one collected over Ir/ZSM-5 (10.0) with Si/Al ratio of 80 shows the highest heating value, which is 5.7% higher than that from pure ZSM-5 (80:1). The promotion on the heating value is in line with the H/C

and alkane content enhancements of product oil as shown in Fig. 1 and Fig. 2, which reveals that the olefin saturation under methane environment could make the undesirable product more valuable in term of energy density. As what have been discussed previously, the surface acidity could obviously influence the upgrading performance of olefin to alkane under methane environment. Hence, the effect of different Si/Al ratios of Ir/ZSM-5 catalyst on the heating value of the produced oil is also investigated. As shown in Fig. 3(b), surface acidity of catalysts could obviously exert impact on the heating value of the product oil. The product oil from Ir/ZSM-5 (280:1) exhibits comparable but lower heating value with that from Ir/ZSM-5 (80:1), which aligns with the data from H/C and alkane content measurements. For the product oil of Ir/ZSM-5 (280:1), although the alkane content is very low as shown in Fig. 2(b), the major form of alkene is the long-chain molecule, which is in line with high heating value. These results explain why the product oil from Ir/ZSM-5 (280:1) could exhibit slightly lower heating value compared with that from Ir/ZSM-5 (80:1). However, the heating value of the upgraded oil is significantly dropped when the Ir/ZSM-5 catalyst with Si/Al ratio of 50 is utilized compared with that from Ir/ZSM-5 (80:1), which is probably because the product oil collected over Ir/ZSM-5 (50:1) is mainly composed of short-chain molecules as explained in the last section due to over-cracking.

3.1.4. The effects of hydrogen resources on the olefin upgrading: H₂ and CH₄

Generally, Hydrogen (H₂) is considered as one of the most widely used hydrogen donors for hydrocracking reaction [4,5]. However, the production of H₂ could cause high capital and operation costs as well as greenhouse gas emission due to the process of CH₄ steam reforming. In order to compare the effects of hydrogen donors on the olefin upgrading, the CH₄ and H₂ are chosen to investigate their effects on the heating value and alkane content of the product oil generated over Ir/ZSM-5 (10.0) with Si/Al ratio of 80.

As shown in Fig. 4(a), when the reaction temperature is set at 400 °C, the heating value of product oil formed under H₂ is higher than that under CH₄. However, the heating value of product oil generated under H₂ is lower than that under CH₄ when the reaction temperature is reduced to 350 °C. Generally speaking, the product oil formed under CH₄ is comparable with that under H₂ in term of heating value, indicating that methane might be able to act as alternative hydrogen donor for catalytic hydrocracking under appropriate reaction conditions. As shown in Fig. 4(b), the alkane content of the oil product is 57.5 ± 7.4% when H₂ is used at 400 °C, which is higher than that (44.2 ± 2.4%) produced under the environment of CH₄. However, the alkane content of the product oil is dropped to 49.5 ± 8.6% under the H₂ atmosphere at 350 °C, which is significantly lower than that (83.8 ± 2.1%) generated when CH₄ is charged. As a result, the alkane content of product oil further confirms that comparable or even better catalytic performance for the olefin upgrading could be achieved under the environment of CH₄ and also indicates that the low-cost methane might have the potential to be widely utilized as the hydrogen donor instead of expensive hydrogen (H₂) when appropriate catalyst is used.

3.2. Structural characterizations

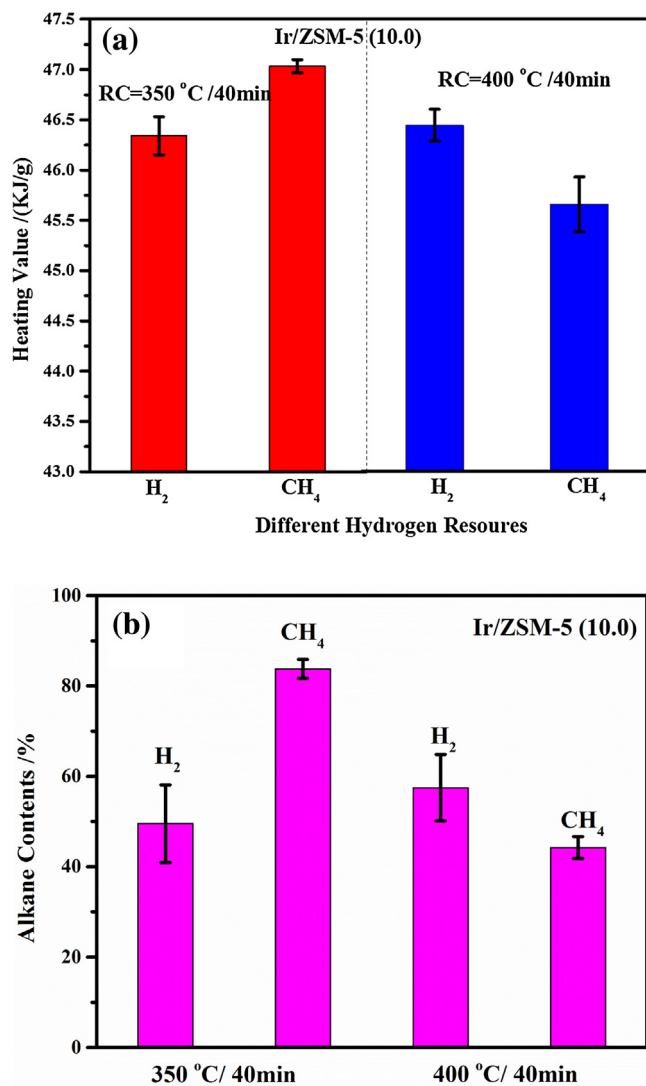
3.2.1. Surface area and crystalline structure

As shown in Fig. 5, there are two characteristic doublet and triplet peaks of pure ZSM-5, located at 8.0, 8.8, 23.1, 23.9 and 24.4°, which indicates that the ZSM-5 support is highly crystalline [49]. All of the Ir/ZSM-5 samples display the typical structure of pure ZSM-5. However, the changes on the peak intensity ratio of doublet and triplet peaks indicate the symmetry of original characteristic peaks have been slightly altered [46] probably due to the Ir intro-

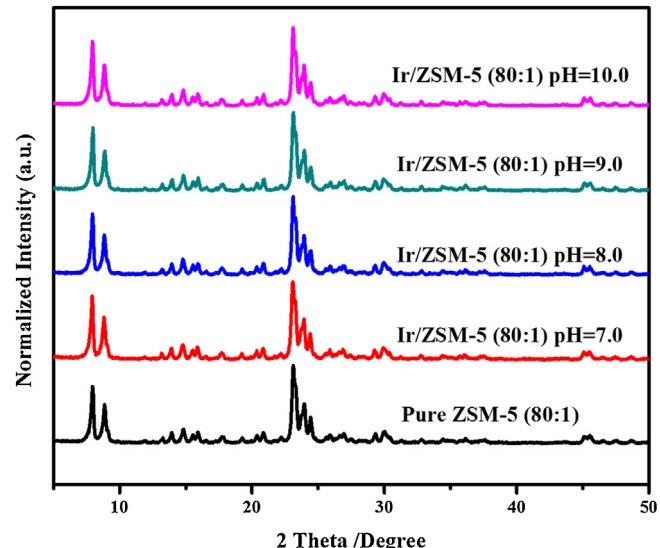
Table 2

The textural properties of Ir/ZSM-5 (80:1) and ZSM-5 (80:1) catalysts.

Samples	BET Surface Area (m^2/g)			Porous Volume (cm^3/g)			Pore Size (nm)
	External	Microporous	Total	Microporous	Mesoporous	Total	
Pure ZSM-5	125.7	235.6	361.4	0.124	0.196	0.321	3.5
Ir/ZSM-5 (10.0)	139.7	253.8	393.5	0.134	0.246	0.380	3.9
Ir/ZSM-5 (9.0)	110.0	292.4	402.4	0.124	0.100	0.224	2.2
Ir/ZSM-5 (8.0)	110.9	302.8	413.7	0.129	0.104	0.233	2.3
Ir/ZSM-5 (7.0)	89.3	315.8	405.1	0.134	0.078	0.212	2.1

**Fig. 4.** Effects of H₂ and CH₄ on the heating value (a) and alkane content (b) of the product oil collected from Ir/ZSM-5 (10.0).

duction. No diffraction peaks of iridium are observed, owing to the facts that the Ir content in the catalyst is low and the Ir species might be highly dispersed on the support. The deposition of iridium does not induce significant changes in the lattice parameter of ZSM-5 but modifies the porous properties of Ir/ZSM-5 catalysts, as listed in Table 2. The BET surface area, porous volume and size of Ir/ZSM-5 catalysts are significantly changed compared with that of pure ZSM-5. The changes on the porous size might be attributed to dispersion of Ir particles and the dissolution of Si because alkaline solutions are used to prepare the catalysts [50,51]. Especially, the porous size and volume of Ir/ZSM-5 (10.0) sample is increased compared with that of pure ZSM-5, which may allow more molecules to get access to the active sites located in the internal porous struc-

**Fig. 5.** XRD patterns of pure ZSM-5 and Ir/ZSM-5 prepared under different pH values.

ture and thus benefit the enhancement of the catalytic performance toward 1-decene upgrading under methane environment.

3.2.2. HRTEM of Ir/ZSM-5 (10.0) catalyst

Due to the low loading of Ir, it is very difficult to detect Ir by XRD method. Therefore, HRTEM is used to identify the present status of Ir on the surface of Ir/ZSM-5 (10.0) presented in Fig. 6(a–c). As shown in Fig. 6(a), the Ir particles are evenly dispersed on the surface of ZSM-5 and the distribution of particle size is very narrow. The mean size of Ir particles is 1.3 nm as shown in the inset image. The Ir particles seem to be aggregated particles from the low-magnification TEM image while the zoomed image exhibits that Ir particles are anchored in the form of independent particles like a flower on the surface of ZSM-5 as shown in Fig. 6(b). The images of HRTEM clearly indicate that the Ir species are highly dispersed on the surface of ZSM-5. After reaction, the Ir particle size is increased to 4.2 nm as shown in Fig. 6(d), which might be derived from the agglomeration of highly dispersed particles under the reaction conditions of high temperature and high pressure.

C–H bond dissociation determines CH₄ conversion rates on the surface of Ir [47,48], which mainly depends on the dispersion of Ir [29]. Hence, the cleavage of C–H bond of methane could be greatly facilitated by the highly dispersed Ir particles. Furthermore, Ir particles with lattice fringes of 2.1 Å corresponding to Ir (111) [52] are observed in the HRTEM image of Ir/ZSM-5 (10.0) as shown in Fig. 6(c). Methane could be efficiently activated on the Ir (111) surface since the activation energy for methane dissociative chemisorption could be as low as 15 kJ/mol [35,53]. The significant increases of the H/C ratio and alkane content as well as heating value of the product oil collected over Ir/ZSM-5 sample compared to those from pure ZSM-5 confirm that the highly dispersed Ir particles could promote the methane activation and thus generate sufficient

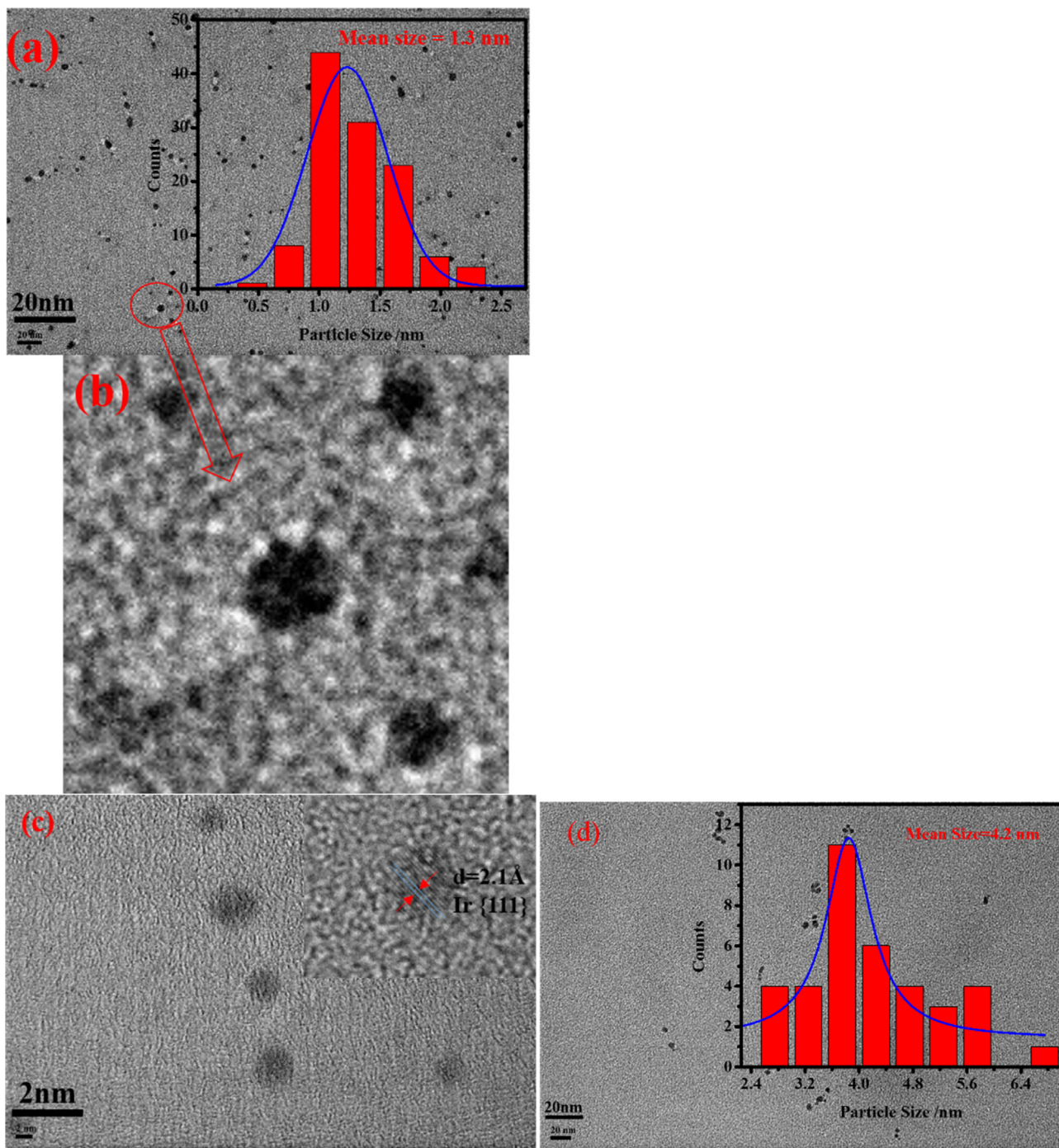


Fig. 6. TEM pictures of Ir/ZSM-5 (10.0) fresh: low-magnification TEM image (a); image of zoomed area (b) and high-magnification TEM image (c); low-magnification TEM image of Ir/ZSM-5 (10.0) used (d); Inset image: statics data about particle size distribution of Ir; The scale bar of (a) and (d) was 20 nm. The scale bar of (c) was 2 nm.

hydrogen resources for the saturation of cracked fragments from olefin, which is thought to be the key factor for olefin upgrading under methane environment [10,54,55].

3.2.3. Nuclear magnetic resonance of Si and Al (^{29}Si and $^{27}\text{Al-NMR}$)

Fig. 7(a) and (b) show the changes on coordination environment of Al and Si species of pure ZSM-5 and Ir/ZSM-5 (10.0). The ^{29}Si NMR spectra of pure ZSM-5 exhibit two overlapping signals at the chemical shifts of -112 and -105 ppm. The band at -112 ppm is assigned to $\text{Q}^4[\text{Si}(\text{OSi})_4]$ species, and the band at -105 ppm is assigned to silicon-oxygen tetrahedron (SiO_4) surrounded by three SiO_4 and

one aluminum-oxygen tetrahedron (AlO_4^-), normally denoted as $\text{Si}(3\text{Si}, 1\text{Al})$ [56]. For the ^{29}Si NMR spectra of Ir/ZSM-5 (10.0), the increased intensity of signal at -105 ppm could be attributed to more AlO_4^- species present in the framework of zeolites [43,56]. According to the ^{29}Si MAS NMR results, the ratio of silicon to framework aluminum in the ZSM-5 zeolites is estimated using the equation [57,58] $(\text{Si}/\text{Al})_{\text{NMR}} = I/\sum 0.25nI_n$, where I denotes the sum of the peak areas of the NMR signals assigned to the $\text{Si}(n\text{Al})$ building unit, and I_n represents the intensity of the resonance corresponding to the $(\text{AlO})_n\text{Si}(\text{OSi})_{4-n}$ sites. The ratio of Si/Al_F (F : Framework) is decreased from 51 of pure ZSM-5 to 39 of Ir/ZSM-5 (10.0), sug-

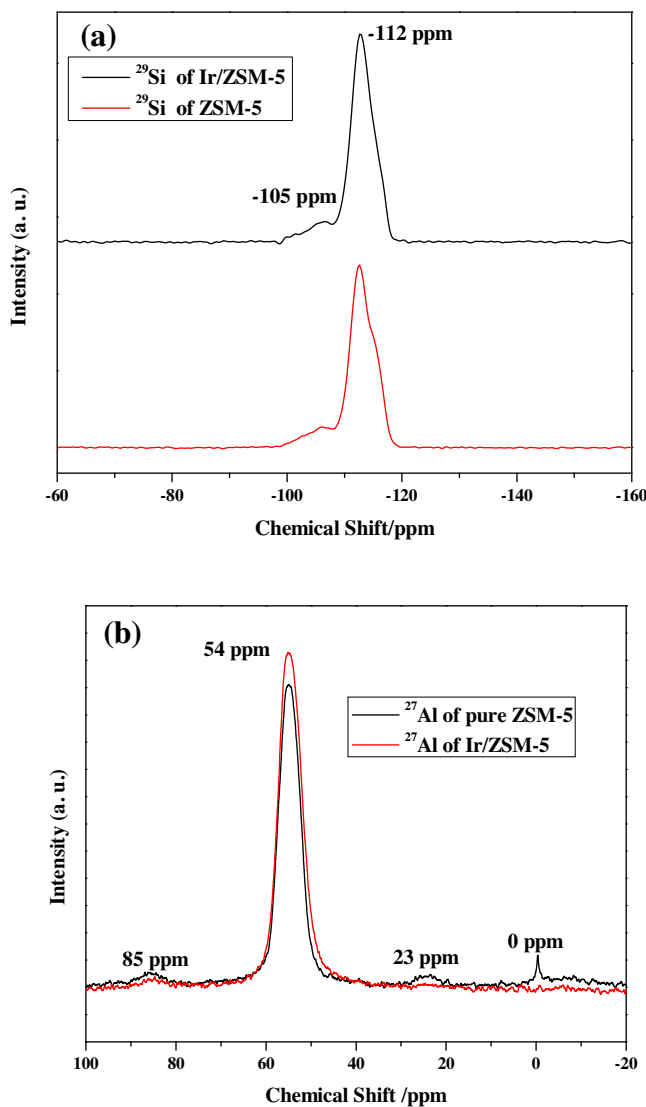


Fig. 7. NMR of pure ZSM-5 and Ir/ZSM-5 (10.0): ^{29}Si (a) and ^{27}Al (b).

gesting that the amount of framework Al has been increased from 1.8 wt.% (pure ZSM-5) to 2.4 wt.% (Ir/ZSM-5 (10.0)).

For the ^{27}Al NMR spectra of pure ZSM-5 (80:1), the peaks at 54 ppm and 0 ppm can be correspondingly assigned to tetrahedrally coordinated framework aluminum and octahedral extra-framework aluminum [59–62]; the resonance peaks at 85 ppm and 23 ppm are assigned to spinning sideband due to the resonance at 54 ppm. The disappearance of the signal at 0 ppm demonstrates that the octahedrally coordinated aluminum is transformed into the tetrahedrally coordinated Al [59], combined with the data of ^{29}Si NMR spectra. Obviously, both of ^{27}Al and ^{29}Si NMR spectra confirm that non-framework aluminum is transformed into the framework Al [63–65]. One of the possible mechanisms for the transformation of non-framework aluminum species into the framework of the zeolites is: the non-framework aluminum species occupying the framework vacancies present in the dealuminated zeolites and/or through substitution of aluminum species for the framework silicon atoms [63–65]. Meanwhile, the framework Al of Ir/ZSM-5 shows higher chemical shift about 1.5 ppm compared to that of pure ZSM-5, which indicates that the presence of Ir has modified the coordination environment of Al in the ZSM-5. Correspondingly, the variation on the coordination environment of Al in ZSM-5 after Ir addition suggests the changes on the electronic

structure of Ir due to the interaction between the highly dispersed Ir and Al in the ZSM-5.

3.2.4. X-ray photoelectron spectroscopy (XPS)

XPS spectra are used to probe the surface chemical states of Ir/ZSM-5 as shown in Fig. 8. As demonstrated in Fig. 8(a), Al 2p photoelectron peak at 74.7 eV is attributed to the Al atoms in the framework of ZSM-5, where Al atoms are connected to the bridged O atom in the $-\text{Si}=\text{O}-\text{Al}-$ chain and oxidation states should be +3 [66]. After Ir deposition, the binding energy (BE) of Al 2p shifts to lower energy by 0.3 eV. Meanwhile, the binding energy of O 1s shifts to lower energy by 0.2 eV after Ir deposition as shown in Fig. 8(b). The peak of O 1s might originate from IrO_2 and/or SiO_2 in the framework of zeolite support [67–70]. The changes of binding energies of Al and O further suggest the presence of strong electronic interaction between highly dispersed Ir and ZSM-5.

Quantitative deconvolution of the Ir 4f lines contains two peaks, corresponding to $\text{Ir } 4\text{f}_{7/2}$ and $\text{Ir } 4\text{f}_{5/2}$. Due to the low loading of Ir, only the peak of $\text{Ir } 4\text{f}_{5/2}$ is observed as shown in Fig. 8(c). For the fresh Ir/ZSM-5 (10.0) catalyst, the peak is located at 64.5 eV, which aligns with the standard binding energy of IrO_2 (64.8 eV) [67–70]. The formation of IrO_2 might originate from the high-temperature calcination in air, which oxidizes the highly dispersed Ir particles into IrO_2 . XPS data suggests the main composition of active Ir species for methane activation is the IrO_2 although the HRTEM data indicates that there might be a small proportion of Ir species in the form of metallic Ir, both of which could show excellent capability for methane activation [3,31–35]. Furthermore, for the spent Ir/ZSM-5 catalysts, the binding energy of $\text{Ir } 4\text{f}_{5/2}$ is shifted to 64.2 eV, which indicates the slight reduction of IrO_2 species during reaction. This further confirms the importance of IrO_2 for methane activation in the reaction of olefin upgrading. IrO_2 could exhibit very high reactivity for methane activation because the electron density transfer from the d_{z^2} orbital of coordinatedly unsaturated Ir (Ir_{cu}) atom to C–H bond could weaken the C–H bond of CH_4 through the interaction between the σ bond of C–H of CH_4 and the Ir_{cu} atoms according to the literature [33]. Hence, the abstraction of first hydrogen atom from CH_4 would be much easier over Ir/ZSM-5, which could significantly promote methane activation [32].

3.2.5. DRIFT spectra of pyridine adsorption

Fig. 9 shows a comparative result of acidities obtained from FT-IR analyses. It can be seen that both of the Brønsted acid (B) and Lewis (L) acid exist in the catalysts of pure ZSM-5 and Ir/ZSM-5 (10.0), based upon the peaks at around 1540 and 1450 cm^{-1} , respectively; As for the peak at 1490 cm^{-1} , it can be ascribed to pyridine adsorption on the Lewis sites as well as on Brønsted acid sites [71]. It is obvious that the peak area with Ir/HZSM-5 (10.0) is larger than that of pure ZSM-5, which indicates a higher concentration of acid sites in the catalyst of Ir/HZSM-5 (10.0). The concentration of Brønsted acid and Lewis acid sites can be calculated from the integrated peak area of the Brønsted acid and Lewis acid bands [72]. The relative ratio of B/L is increased from 12.2% (pure ZSM-5) to 19.3% (Ir/ZSM-5 (10.0)), which is consistent with the NMR data as shown in Fig. 7 and further suggests that more framework Al species are formed in Ir/ZSM-5 (10.0) [57]. The increase of the surface Brønsted acidic sites of Ir/ZSM-5 catalysts should mainly originate from the increased concentration of tetrahedral framework aluminum due to the transformation of extra-framework aluminum into the tetrahedrally coordinated Al as shown in ^{27}Al NMR data. The increase of Lewis acid sites can be ascribed to the highly dispersed Ir species since previous research confirms that the highly dispersed metal species could increase Lewis acid sites by interacting with the acidic protons (Brønsted acid sites) of the zeolite framework [73,74].

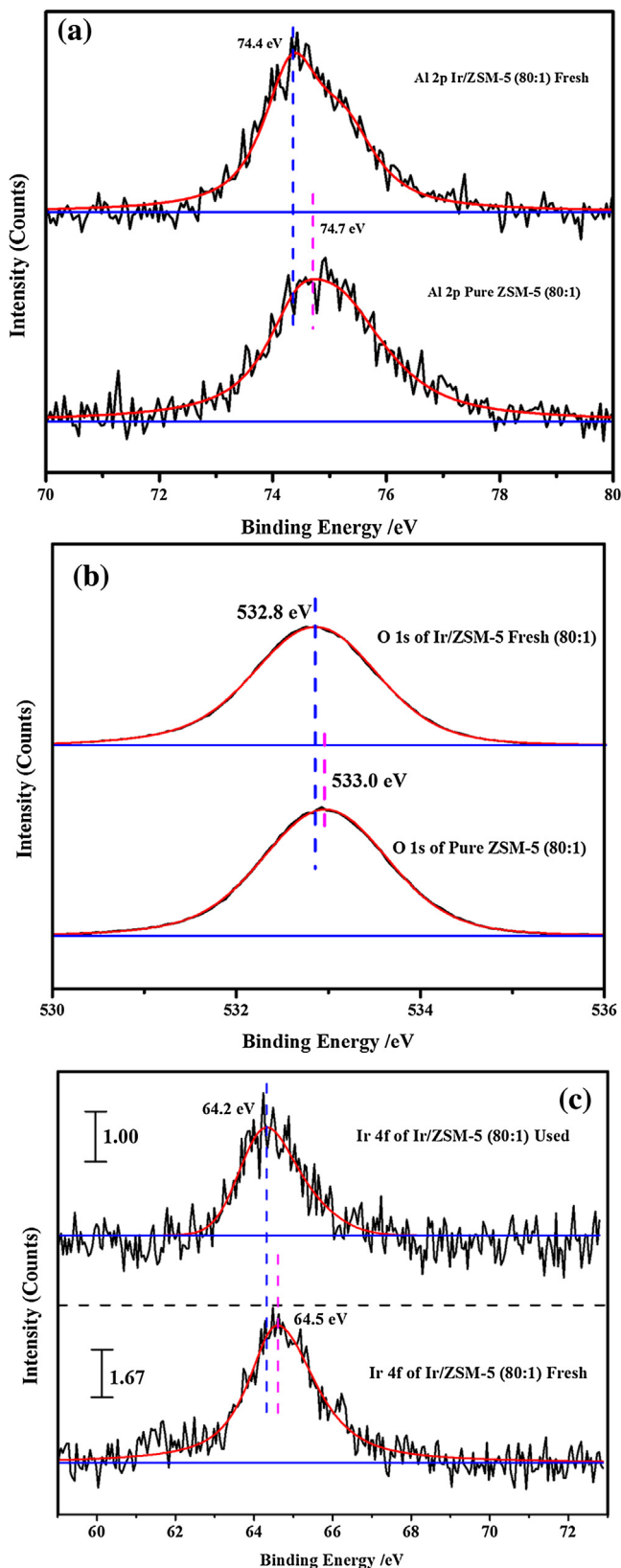


Fig. 8. The XPS spectra of Pure ZSM-5 and Ir/ZSM-5 (10.0): Al 2p (a); O 1s (b) and Ir 4f (c).

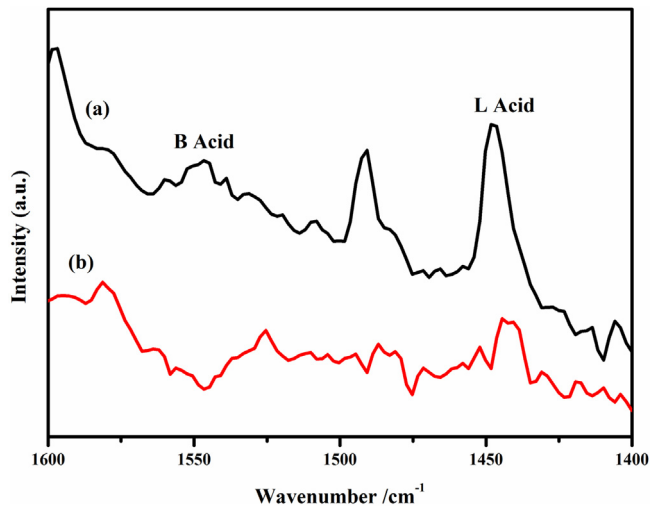


Fig. 9. FT-IR spectra after the adsorption of pyridine followed with desorption at 350 °C of Ir/ZSM-5 (10.0) (a) and pure ZSM-5 (b).

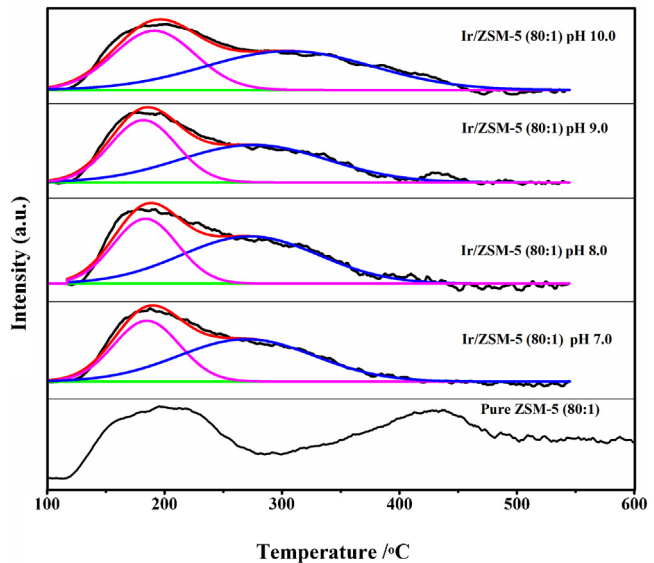


Fig. 10. NH₃-TPD profiles of pure ZSM-5 and Ir/ZSM-5 (80:1) prepared under different pH values.

3.2.6. NH₃-Temperature programmed desorption (NH₃-TPD)

Surface acidic centers could provide protons to protonate the alkene through hydrogen transfer from the ZSM-5 support on which the carbenium ions are formed [20,43,75–77]. The formation of carbenium ions is the crucial step for further reactions like C–C scission, agglomeration, isomerization, cyclization, hydrogen redistribution and so on [24–26]. Shortly, surface acidic centers of bifunctional catalysts play important roles on olefin upgrading in the aspects of hydrogen transfer [10,43] and the stabilization of carbenium intermediates produced from cracked olefins [13,78].

Fig. 10 shows that there are two obvious NH₃ desorption peaks from pure ZSM-5, referred as weak surface acidic sites in low temperature region (LT, maximum peak at 196 °C) and strong surface acidic sites in high temperature region (HT, maximum peak at 436 °C) [79–81]. Compared with that from pure ZSM-5, the HT NH₃ desorption peak disappears when the Ir/ZSM-5 catalysts are charged, which suggests the original strong acid sites are occupied

by the IrO_x species; alternatively, there is a new peak centered at $284\sim295^\circ\text{C}$ forming over all of the Ir/ZSM-5 catalysts during NH_3 desorption process, which can be attributed to the acid sites, originating from the highly dispersed IrO_x species interacting with the Brønsted acid sites in the ZSM-5. Previous reports studying Zn and Ga-modified zeolites also find that the highly dispersed $(\text{GaO})^+$ and ZnO species could occupy the strong acid sites and generate new acid sites by interacting with the acidic protons (Brønsted acid sites) of the zeolite framework [73,74].

The desorption temperature and peak area of NH_3 -TPD profiles could directly reflect the information about the strength and amount of surface acidity [79], respectively. If the amount of surface acidity of pure ZSM-5 at low-temperature region is taken as the baseline value (1.00), the amount of LT NH_3 desorption peak of all of the Ir/ZSM-5 catalysts is lower than that of pure ZSM-5, which could be ascribed to the dealumination during the process of catalysts synthesis [82]. Meanwhile, the temperature of LT NH_3 desorption peak of Ir/ZSM-5 samples is shifted down about 10°C from 191°C (pure ZSM-5), implying that the strength of surface acidity is decreased. However, the total amount of surface acid sites of Ir/ZSM-5 samples is increased compared with that of pure ZSM-5, which might be ascribed to the increase of four-coordinate framework aluminum as shown in NMR data and the contribution from highly dispersed Ir species. These results indicate that the deposition of Ir efficiently modulates the surface acidity of Ir/ZSM-5 catalysts. The detailed desorption temperature and peak area of NH_3 -TPD profiles of different catalysts are summarized in Table 3.

The presence of acidic sites could promote the cracking activity through protonation of reactive species and formation of carbenium intermediates [43]. And then, the highly reactive carbenium-ions-derived fragments could be hydrogenated in the presence of hydrogen donors over metallic sites. Metal species incorporated in the framework of zeolites could produce higher concentration of hydrogen acceptor species, which would facilitate the transfer of activated methane [83] and thus accelerate the reaction between activated methane and carbenium-ions-derived fragments.

3.3. Mechanistic discussion

Since iridium is both expensive and rare, the potential industrial application of this process makes it essential to reduce Ir loading on the catalysts. Therefore, we have successfully prepared the evenly dispersed Ir particles on the surface of ZSM-5 through finely tuning the synthesis parameters. The Ir/ZSM-5 catalysts with low Ir loadings have not only enhanced the dispersion and tuned the electronic structure of Ir species but also effectively modulated the surface acidity of ZSM-5, which simultaneously promotes the activation of methane and appropriately tunes the cracking of olefin, thus leading to the performance enhancement of the olefin upgrading under methane environment.

The first hydrogen atom abstraction from methane is the crucial step for supplying hydrogen to saturate the highly active carbenium ions produced from olefin cracking [84]. However, due to the high-symmetry and nonpolar geometric structure, the CH_4 molecule is neither electron donor nor acceptor; the symmetric structural and electronic features of methane molecule make it weakly interacted with catalytic surfaces, which is further confirmed by DFT calculations that interactions (or no interaction) between methane and transition metal surfaces are quite weak [8,9]. However, Ir species could show outstanding capability for methane activation [8,32,33]. Wang et al. [33] reports that the adsorption energy of methane over IrO_2 surface could be -0.63 eV , which is the highest adsorption energy in heterogeneous catalytic system. From a kinetic point of view, a higher adsorption energy of reactants would

lead to a higher turnover frequency in heterogeneous catalytic reactions. In addition, the first hydrogen atom abstraction from methane molecule on the IrO_2 surface is a reaction with relatively low reaction barrier and high exothermic features [33]. The lower reaction barrier than the desorption energy indicates that the IrO_2 surface could provide not only high sticking coefficient but also high turnover frequency in methane dissociation reaction. Furthermore, as shown in HRTEM data, there might be a small proportion of Ir species in the form of metallic Ir, which could also activate methane with the activation energy for methane dissociative chemisorption as low as 15 kJ/mol [35]. The enhancements on the H/C atomic ratio and alkane content of product oil as well as heating value improvement indicate that the Ir species over ZSM-5 significantly promote the activation of methane, which would supply sufficient hydrogen for the saturation of carbenium ions derived from the cracked alkene.

For the catalytic cracking reaction of alkene, it is generally agreed that the active centers in these reactions are the protonic acidic sites on the surface of catalysts and the reactive species are the carbenium ions [20,43,75,76]. Generally speaking, the general mechanism of alkene cracking over bifunctional hydrocracking catalysts involves three stages [20]: the formation of carbenium ions over acidic centers, cracking of alkenes over acidic centers through the carbenium-ion mechanism and catalytic hydrogenation of the cracked products (low-molecular-weight alkenes) to alkanes over the metal. The reaction of 1-alkene with linear chain ($\text{CH}_2=\text{CH}-\text{R}$) produces the secondary carbenium ion ($\text{CH}_3^+ \text{CH}-\text{R}$). The zeolitic acidity plays a very important role on the cracking and cyclization [24] since the formation of carbenium ions needs the H^+ from the ZSM-5 support [77]. The transformation of extra-framework Al into the framework Al efficiently increases the amount of surface B and L acidic sites as proved by the aforementioned Pyridine FT-IR, NMR and NH_3 -TPD data. The increase of surface acidity intensity indicates that more H^+ species could be supplied for the formation of carbenium ions, which significantly accelerates the catalytic cracking.

In the absence of hydrogen donors, reactions of alkene cracking are often accompanied with the formation of limited saturated alkanes through abstracting the hydrogen from the alkenes, which leads to the main products of aromatics in order to keep hydrogen balanced [85]. This explains why there are still a few alkanes and abundant aromatics formed on the pure ZSM-5. However, if the cracking is carried out in the presence of hydrogen donors, unsaturated products could be hydrogenated over metal centers [20]. Due to the synergistic effects of Ir/ IrO_2 , the dissociation of C–H bond of CH_4 becomes much easier and therefore more hydrogen could be supplied for the saturation of unsaturated products, which explains why the contents of alkanes in the product oil are greatly increased over Ir/ZSM-5 catalysts.

Generally speaking, aromatization occurs on the acidic sites of zeolites via carbocation intermediates starting with cracking of long-chain olefins into ones with shorter chain, condensation of carbenium ions and alkene molecules, ring enlargement via protonated cyclopentenyl ions and then the dehydrocyclization [23–26]. The precursor of aromatics is cyclopentenyl ion [26]. Since the produced alkanes after upgrading are mainly cyclopentane-derived compounds as listed in Table 1, the formation mechanism of cycloalkane in this study might be similar with that of aromatics. A hypothetic scheme for this reaction is proposed in Fig. 11 for better illustrating the involved reaction mechanism. As can be clearly seen, the significant difference between this study and previous researches on aromatization is that the process of dehydrocyclization is obviously suppressed during olefin upgrading under methane environment with Ir/ZSM-5 charged because the promotion of methane activation over Ir/ IrO_2 could supply sufficient hydrogen for the

Table 3

Summary of surface acidity of different samples.

Catalysts	Peak 1		Peak 2		Peak 3		Total
	Amount ^a	Temp. (°C)	Amount	Temp. (°C)	Amount	Temp. (°C)	
Ir/ZSM-5 pH 7.0	0.65	177	0.94	256	/	/	1.59
Ir/ZSM-5 pH 8.0	0.67	176	1.04	257	/	/	1.71
Ir/ZSM-5 pH 9.0	0.74	174	0.99	258	/	/	1.73
Ir/ZSM-5 pH 10.0	0.97	182	1.31	285	/	/	2.29
Pure ZSM-5	1.00	191	/	/	0.63	413	1.63

^a Amount of surface acidity reported here means the relative surface acidity referred to that of pure ZSM-5 (80:1) at low-temperature region. The intensity of surface acidity of pure ZSM-5 (80:1) was taken as the standard (1.00). Before calculating, the curve of empty experiment was subtracted as the baseline from the NH₃-TPD profiles.

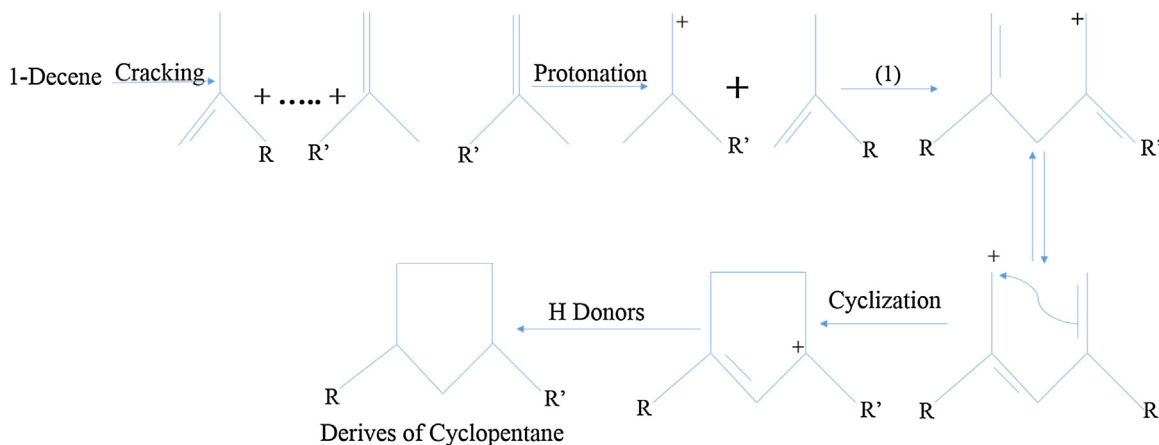


Fig. 11. Proposed scheme for the generation of cyclopentane-derived compounds from 1-decene upgrading under methane environment. (1): Deprotonation and hydride transfer [25].

saturation of the formed cyclopentenyl ion intermediates and its further alkylation, which could offer alternative reaction pathways, inhibiting the dehydrogenation reaction for aromatics formation [86].

Due to the complexity and importance of the long-chain olefin cracking, the further research about the detailed mechanism of cyclization is ongoing in our group.

4. Conclusions

The saturation of olefin plays a very important role on enhancing the quality of synthetic oil in terms of long-term storage and environmental protection. From the results discussed above, it can be concluded that the methane might have the potential to replace the conventional H₂ as the novel hydrogen donor for olefin upgrading. Methane as the hydrogen donor could show the comparable catalytic performance as that of hydrogen (H₂), which could efficiently reduce not only the capital and operation costs but also the greenhouse gas emissions during petroleum refining. In reality, such reductions are challengeable without addition of an effective catalyst. The highly dispersed Ir particles on ZSM-5 synthesized at appropriate pH condition with suitable Si/Al ratio developed in this research have not only lowered the loading of noble metal and promoted methane activation but also appropriately modulated the surface acidity of ZSM-5, leading to the catalytic performance enhancement of olefin upgrading under methane environment. From the aspect of fine chemicals production, the remaining challenges of using CH₄ as hydrogen donors towards commercialization might be still the selectivity of products. Nevertheless, our research philosophy used in this study might create a novel route for methane utilization, which is beneficial for the wider application of natural gas in chemical industries.

Acknowledgement

We gratefully acknowledge the financial supports from Meg Energy Corp. and Alberta Innovates—Energy and Environment Solutions (AI-EES, 2142).

References

- [1] R. Sadengheibi, 3rd ed., Elsevier, New York, 2012.
- [2] de Klerk, A. Weinheim, Wiley-VCH, Germany, 2011.
- [3] D.C. Leitch, Y.C. Lam, J.A. Labinger, J.E. Bercaw, *J. Am. Chem. Soc.* 135 (2013) 10302–10305.
- [4] A. Hart, G. Leeke, M. Greaves, *J. Wood, Fuel* 119 (2014) 226–235.
- [5] D.C. Longstaff, M.D. Deo, F.V. Hanson, A.G. Oblad, C.H. Tsai, *Fuel* 71 (1992) 1407–1419.
- [6] S.D. Angelis, G. Monteleone, A. Giacconi, A.A. Lemonidou, *Int. J. Hydrogen Energy* 39 (2014) 1979–1997.
- [7] H. Idriss, *Platinum Metals Rev.* 48 (2004) 105–115.
- [8] B. Xing, X.Y. Pang, G.C. Wang, *J. Catal.* 282 (2011) 74–82.
- [9] C.T. Au, C.F. Ng, M.S. Liao, *J. Catal.* 185 (1999) 12–22.
- [10] V.R. Choudhary, A.K. Kinage, T.V. Choudhary, *Science* 275 (1997) 1286–1288.
- [11] V.R. Choudhary, K.C. Mondal, S.A.R. Mulla, *Angew. Chem. Int. Ed.* 44 (2005) 4381–4385.
- [12] O.A. Anunziata, J. Cussa, A.R. Beltramone, *Catal. Today* 171 (2011) 36–42.
- [13] T. Baba, Y. Abe, *Appl. Catal. A: Gen.* 250 (2003) 265–270.
- [14] D.J. Wang, J.H. Lunsford, M.P. Rosyne, *J. Catal.* 169 (1997) 347–358.
- [15] P. He, H. Song, *Ind. Eng. Chem. Res.* 53 (2014) 15862–15870.
- [16] A. Guo, C. Wu, P. He, Y. Luan, L. Zhao, W. Shan, H. Song, *Catal. Sci. Technol.* 6 (2016) 1201–1213.
- [17] P. He, Y. Lou, H. Song, *Fuel* 182 (2016) 577–587.
- [18] Y. Lou, P. He, L.L. Zhao, H. Song, *Fuel* 183 (2016) 396–404.
- [19] A. Corma, *J. Catal.* 216 (2003) 298–312.
- [20] Y.V. Kissin, *J. Catal.* 163 (1996) 50–62.
- [21] G.A. Olah, D.J. Donovan, *J. J. Am. Chem. Soc.* 99 (1977) 5026–5039.
- [22] Y.V. Kissin, *Catal. Rev.* 43 (2001) 85–146.
- [23] N. Viswanadham, A.R. Pradhan, N. Ray, S.C. Vishnoi, U. Shanker, P.T.S.R. Rao, *Appl. Catal. A: Gen.* 137 (1996) 225–233.
- [24] V.R. Choudhary, S.A.R. Mulla, S. Banerjee, *Micro. Meso. Mater.* 57 (2003) 317–322.
- [25] P. Dejaïve, J.C. Védrine, V. Bolis, E.G. Derouane, *J. Catal.* 63 (1980) 331–345.
- [26] J. Sommer, A. Sassi, M. Hachoumy, R. Jost, A. Karlsson, P. Ahlberg, *J. Catal.* 171 (1997) 391–397.

- [27] E.F. Iliopoulou, E.A. Efthimiadis, L. Nalbandian, I.A. Vasalos, J.O. Barth, J.A. Lercher, *Appl. Catal. B: Environ.* 60 (2005) 277–288.
- [28] W.H. Chen, I. Ermanoski, T. Jacob, T.E. Madey, *Langmuir* 22 (2006) 3166–3173.
- [29] J. Lin, A.Q. Wang, B.T. Qiao, X.Y. Liu, X.F. Yang, X.D. Wang, J.X. Liang, J. Li, J.Y. Liu, T. Zhang, *J. Am. Chem. Soc.* 135 (2013) 15314–15317.
- [30] Y.H. Zhang, Y.D. Wu, H.F. Wang, Y. Guo, L. Wang, W.C. Zhan, Y.L. Guo, G.Z. Lu, *Catal. Commun.* 61 (2015) 83–87.
- [31] J.M. Wei, E. Iglesia, *Angew. Chem. Int. Ed.* 43 (2004) 3685–3688.
- [32] C.C. Wang, S.S. Siao, J.C. Jiang, *J. Phys. Chem. C* 116 (2012) 6367–6370.
- [33] S.L. Liu, Z.Y. Geng, Y.C. Wang, Y.F. Yan, *J. Phys. Chem. A* 116 (2012) 4560–4568.
- [34] F.X. Li, X.G. Zhang, P.B. Armentrout, *Int. J. Mass Spectrom.* 255–256 (2006) 279–300.
- [35] H.L. Abbott, I. Harrison, *J. Phys. Chem. B* 109 (2005) 10371–10380.
- [36] M. Okumura, N. Masuyama, E. Konishi, S. Ichikawa, T. Akita, *J. Catal.* 208 (2002) 485–489.
- [37] L. Wang, Y.H. Zhang, Y. Lou, Y.L. Guo, G.Z. Lu, Y. Guo, *Fuel Process Technol.* 122 (2014) 23–29.
- [38] Y.H. Zhang, Y.F. Cai, Y. Guo, H.F. Wang, L. Wang, Y. Lou, Y.L. Guo, G.Z. Lu, Y.Q. Wang, *Catal. Sci. Technol.* 4 (2014) 3973–3980.
- [39] L. Wang, Y.F. Feng, Y.H. Zhang, Y. Lou, G.Z. Lu, Y. Guo, *Fuel* 96 (2012) 440–445.
- [40] S.J. Lee, A. Gavriilidis, *J. Catal.* 206 (2002) 305–313.
- [41] Y. Lou, J. Ma, X.M. Cao, L. Wang, Q.G. Dai, Z.Y. Zhao, Y.F. Cai, W.C. Zhan, Y.L. Guo, P. Hu, G.Z. Lu, Y. Guo, *ACS Catal.* 4 (2014) 4143–4152.
- [42] Y. Lou, X.M. Cao, J.G. Lan, L. Wang, Q.G. Dai, Y. Guo, J. Ma, Z.Y. Zhao, P. Hu, G.Z. Lu, *Chem. Commun.* 50 (2014) 6835–6838.
- [43] G.L. Zhao, J.W. Teng, Z.K. Xie, W.Q. Jin, W.M. Yang, Q.L. Chen, Y. Tang, *J. Catal.* 248 (2007) 29–37.
- [44] G.L. Zhao, J.W. Teng, Y.H. Zhang, Z.K. Xie, Y.H. Yue, Q.L. Chen, Y. Tang, *Appl. Catal. A* 299 (2006) 167–174.
- [45] J. Lopez-Gejo, J.T. Kunjappu, J. Zhou, B.W. Smith, P. Zimmerman, W. Conley, N. Turro, *J. Chem. Mater.* 19 (2007) 3641–3647.
- [46] D.R. Lide, CRC Press, Boca Raton, FL, 2004.
- [47] M. Conte, J.A. Lopez-Sanchez, Q. He, D.J. Morgan, Y.L. Ryabenkova, J.K. Bartley, A.F. Carley, S.H. Taylor, C.J. Kiely, K. Khalid, G.J. Hutching, *J. Catal. Sci. Technol.* 2 (2012) 105–112.
- [48] A. de Lucas, J.L. Valverde, P. Sanchez, F. Dorado, M.J. Ramos, *Ind. Eng. Chem. Res.* 43 (2004) 8217–8225.
- [49] J.W. Li, H.F. Ma, Q.W. Sun, W.Y. Ying, D.Y. Fang, *Fuel Process. Technol.* 134 (2015) 32–38.
- [50] P.V. Brady, J.V. Walther, *Geochim. Cosmochim. Acta* 53 (1989) 2823–2830.
- [51] V. Lehmann, *Phys. Stat. Sol.* 204 (2007) 1318–1320.
- [52] W. Chen, S.W. Chen, *J. Mater. Chem.* 21 (2011) 9169–9178.
- [53] G. Henkelman, H. Joónsson, *Phys. Rev. Lett.* 86 (2001) 664–667.
- [54] J.H. Lunsford, P. Qiu, M.P. Rosyne, Z.Q. Yu, *J. Phys. Chem. B* 102 (1998) 167–173.
- [55] J.H. Lunsford, M.P. Rosyne, C.E. Smith, M.T. Xu, Z.Q. Yu, *J. Phys. Chem.* 99 (1995) 12581–12587.
- [56] P. Tynjälä, T. Pakkanen, *T. Micro. Meso. Mater.* 20 (1998) 363–369.
- [57] C.H. Song, M. Wang, L. Zhao, N.H. Xue, L.M. Peng, X.F. Guo, W.P. Ding, W.M. Yang, Z.K. Xie, *Chin. J. Catal.* 34 (2013) 2153–2159.
- [58] G. Engelhardt, U. Lohse, E. Lippmaa, M. Tarmak, M.Z. Magi, *Anorg. Allg. Chem.* 482 (1981) 49–64.
- [59] F. Pan, X.C. Lu, Q.S. Zhu, Z.M. Zhang, Y. Yan, T.Z. Wang, S.W. Chen, *J. Mater. Chem. A* 2 (2014) 20667–20675.
- [60] W.P. Guo, C.R. Xiong, L.M. Huang, Q.Z. Li, *J. Mater. Chem.* 11 (2001) 1886–1890.
- [61] J.H. Kwak, J.Z. Hu, D.H. Kim, J. Szanyi, C.H.F. Peden, *J. Catal.* 251 (2007) 189–194.
- [62] F. Deng, Y.R. Du, C.H. Ye, J.Z. Wang, T.T. Ding, H.X. Li, *J. Phys. Chem.* 99 (1995) 15208–15214.
- [63] Z. Zhang, X. Liu, Y. Xu, R. Xu, *Zeolites* 11 (1991) 232–238.
- [64] T. Sano, Y. Uno, Z.B. Wang, C.H. Ahn, K. Soga, *Micro. Meso. Mater.* 31 (1999) 89–95.
- [65] H. Hamdan, B. Sulikowski, J. Klinowski, *J. Phys. Chem.* 93 (1989) 350–356.
- [66] K.V.R. Chary, C.P. Kumar, D. Naresh, T. Bhaskar, Y. Sakata, *Appl. Catal. A: Gen.* 243 (2006) 149–157.
- [67] I.G. Casella, M. Contursi, R. Toniolo, *J. Electroanal. Chem.* 736 (2015) 147–152.
- [68] S.I. Vot, L. Rouei, D. Beilanger, *Electrochim. Acta* 59 (2012) 49–56.
- [69] L.A. Silva, V.A. Alves, S.C. de Castro, J.F.C. Boodts, *Colloids Surf. A* 170 (2000) 119–126.
- [70] Y.X. Liu, H. Masumoto, T. Goto, *Mater. Trans.* 45 (2004) 900–903.
- [71] O. M'Ramadj, D. Li, X.Y. Wang, B. Zhang, G.Z. Lu, *Catal. Commun.* 8 (2007) 880–884.
- [72] C.J. Liu, K.L. Yu, Y.P. Zhang, X.L. Zhu, F. He, B. Eliasson, *Appl. Catal. B: Environ.* 47 (2004) 95–100.
- [73] H. Xiao, J.F. Zhang, X.X. Wang, Q.D. Zhang, H.J. Xie, Y.Z. Han, Y.S. Tan, *Catal. Sci. Technol.* 5 (2015) 4081–4090.
- [74] O.A. Anunziata, L.B. Pierella, *Catal. Lett.* 19 (1993) 143–151.
- [75] J. Abbot, P.R. Dunstan, *Ind. Eng. Chem. Res.* 36 (1997) 76–82.
- [76] H.M. Kao, C.P. Grey, K. Pitchumani, P.H. Lakshminarasimhan, V. Ramamurthy, *J. Phys. Chem. A* 102 (1998) 5627–5638.
- [77] A.G. Stepanov, M.V. Luzgin, V.N. Romanikov, K.I. Zamaraev, *Catal. Lett.* 24 (1994) 271–284.
- [78] T. Baba, H. Sawada, *Phys. Chem. Chem. Phys.* 4 (2002) 3919–3923.
- [79] F. Lonyi, J. Valyon, *Micropor. Mesopor. Mater.* 47 (2001) 293–301.
- [80] H.G. Karge, *Stud. Surf. Sci. Catal.* 65 (1991) 133–156.
- [81] Q.G. Dai, S.X. Bai, Y. Lou, X.Y. Wang, Y. Guo, G.Z. Lu, *Nanoscale* 8 (2016) 9621–9628.
- [82] K. Na, S. Alayoglu, R. Ye, G.A. Somorjai, *J. Am. Chem. Soc.* 136 (2014) 17207–17212.
- [83] O.A. Anunziata, G.V.G. Mercado, L.B. Pierella, *Catal. Lett.* 87 (2003) 167–171.
- [84] K.W. Li, B.C. Hou, L. Wang, Y. Cui, *Nano Lett.* 14 (2014) 3002–3008.
- [85] J. Abbot, B.W. Woiciechowski, *J. Catal.* 109 (1988) 274–283.
- [86] K. Liu, S.C. Fung, T.C. Ho, D.S. Rumschitzki, *Ind. Eng. Chem. Res.* 42 (2003) 1543–1550.